Cathodoluminescence spectroscopy of nitrided SiO_2-Si interfaces

A. P. Young[a)]
Department of Electrical Engineering, The Ohio State University, Columbus, Ohio 43210-1272

R. Bandhu
Department of Physics, The Ohio State University, Columbus, Ohio 43210-1272

J. Schäfer[b)]
The Ohio State University, Columbus, Ohio 43210-1272

H. Niimi
Department of Materials Science and Engineering, North Carolina State University, Raleigh, North Carolina 27965

G. Lucovsky
Department of Physics, North Carolina State University, Raleigh, North Carolina 27965

(Received 30 December 1998; accepted 3 May 1999)

We use cathodoluminescence spectroscopy (CLS) to investigate the electronic states of ultrathin gate dielectrics with nitrided SiO_2-Si interfaces, known to improve reliability in advanced complementary metal–oxide–semiconductor devices. The 5 nm thick films investigated were: (i) as-deposited (at 300 °C) structures, (ii) 400 °C hydrogen anneal, (iii) 900 °C rapid thermal anneal (RTA), and (iv) a combination of both anneals. CLS emission energies and intensities versus excitation energy were essentially unchanged for the as-deposited interface compared to non-nitrided plasma-processed interfaces. In the near-infrared, features appear at 0.8 and 1.0 eV, with the 1.0 eV peak Si substrate intensity increasing with increasing depth. From depth variation measurements at higher photon energy, a 3.4 eV peak is also shown to arise from the Si substrate, and a 2.7 eV feature is shown to come from the interface region. After hydrogenation, the CLS is essentially the same as for non-nitrided interfaces, except for an increase in the relative intensity of a broad background luminescence ranging from 1.5 to 2.5 eV. However, the RTA and the combination of the RTA and hydrogenation do not completely suppress emission near 2.0 eV feature as for non-nitrided interfaces. From the behavior of the CLS features, we are able to clearly distinguish between interfacial defects and substrate features, which are significantly reduced by the combined RTA/hydrogen anneal, and features that are not reduced by the annealing procedures. © *1999 American Vacuum Society.* [S0734-2101(99)22804-7]

I. INTRODUCTION

As metal–oxide–semiconductor field effect transistor (MOSFET) device dimensions are scaled into the deep submicron range to achieve higher levels of circuit integration, there must be corresponding decreases in the oxide-equivalent thickness of dielectrics to maintain the current flow needed for device operation. In order to maintain current trends, the thickness of the SiO_2 dielectric in these devices is beginning to approach the direct tunneling regime of $\approx$2.0 nm. Point defects, monolayer roughness, substoichiometric SiO_x, and other interfacial properties now occupy a significant fraction of the overall thickness of the dielectric, dominating their behavior and potentially severely limiting device performance and reliability.[1] By using higher-K dielectrics such as Si_3N_4, TiO_2, or Ta_2O_5, the dielectric layer could be made thicker without sacrificing performance, however, high interface state densities measured when these dielectrics are deposited directly on silicon have prevented their use to date. A combination of an ultrathin dielectric plus a SiO_2 passivation layer may accomplish both goals, by combining the low interface state density of the SiO_2-Si interface with the high dielectric constant material making up the rest of the dielectric film. Controlling such thin layers necessitates an increased understanding and control of the chemical bonding and defect states in the immediate vicinity of the underlying SiO_2-Si interface.

Implicit in the deposition process for these composite gate dielectrics is the necessity to combine controlled interface formation either by thermal or plasma-assisted oxidation with physical, chemical vapor, or plasma-assisted deposition processes for the remainder of the dielectric layer. Studies performed to date on SiO_2-Si interfaces and nitrided SiO_2-Si interfaces, have demonstrated that transitions regions with suboxide bonding are created during thermal, rapid thermal or plasma-assisted oxidation, and that to date, the extent of these regions is decreased significantly after a 900 °C anneal.[2] Here, we present results using low-energy cathodoluminescence spectroscopy (CLS) to probe the electronic states associated with incomplete bonding in these transition regions.

a)Corresponding author; electronic mail: apyoung@ee.eng.ohio-state.edu
b)Current address: Lawrence Berkeley Lab, 1 Cyclotron Rd., Mail Stop 7-222, Berkeley, CA 94720.

II. EXPERIMENT

In this work, we report CLS studies of: (i) as-deposited films, (ii) post-deposition hydrogenation for 30 min at 400 °C,[3] (iii) rapid thermal annealing to 900 °C, and (iv) films subjected to a 900 °C rapid thermal anneal followed by hydrogenation at 400 °C.[4,5]

The films were prepared on ~10 Ω cm boron-doped *p*-Si(100) substrates, cleaned by repeated oxidation, then etch back in hydrofluoric acid, with a final oxide-removal etch in 1 at % HF. The SiO_2–Si structures were formed by a three-step plasma process:[6–8] (i) remote plasma-assisted oxidation (RPAO) to form the interface and grow ~0.5–0.6 nm of SiO_2; (ii) remote plasma nitride deposition [1 monolayer of N as measured by Auger electron spectroscopy (AES) and secondary ion mass spectroscopy (SIMS) of similar specimens][9] using N_2 as the source gas; and (iii) remote plasma-enhanced chemical vapor deposition (RPECVD) to deposit the bulk oxide film, to a total SiO_2 thickness of ~5 nm. For each step, the substrate temperature was 300 °C, the process pressure 0.3 Torr, and the plasma power 30 W. The active species for the RPAO were extracted from a remote He/O_2 (10:1) plasma. For the 5 nm oxide film deposition, silane diluted in He (2%) was delivered downstream, and the He/O_2 mixture was excited in the plasma tube. The ratios of the source gases were $He/O_2/SiH_4$=200/20/0.2. For annealing studies, samples were subjected to either a 400 °C anneal in forming gas (N_2/H_2) for 30 min, a rapid thermal anneal (RTA) at 900 °C in Ar for 30 s, or both the RTA and then the 400 °C N_2/H_2 anneal. The specimens were transferred in air into an ultrahigh vacuum (UHV) chamber for CLS analysis. CLS studies were carried out at room temperature with electron beam energies between 0.6 and 4.5 kV and beam currents of 1–4 μA on a spot defocused to approximately 200–500 μm in diameter. The luminescence was recorded with a Leiss flint prism monochromator set to ~40 meV resolution using a Ge detector for infrared energies, and a S-20 photocathode for the visible to near ultraviolet spectral range. The spectra have not been corrected for the optical response of the detection system. It is known however, that for the S-20 detector, the system response is relatively flat from 1.75 to 3.5 eV, while for the Ge detector, the system response curve peaks at 0.85 eV with good sensitivity between 0.75 and 1.35 eV.

III. DEPTH DEPENDENCE

In an attempt to correlate the depth dependence of the electron beam penetration with the primary beam energy, we follow the work of Koyama as reported by Yacobi, who derived an analytical expression for the electron range, assuming a continuous slowing down process for the electrons.[10]

$$R_b = \left(\frac{0.0276A}{\rho Z^{0.889}} \right) E^{1.67} (\mu\text{m}), \tag{1}$$

where A is the atomic mass, ρ is the density in g/cm^3, Z is atomic number, and E is the energy of the incident electron

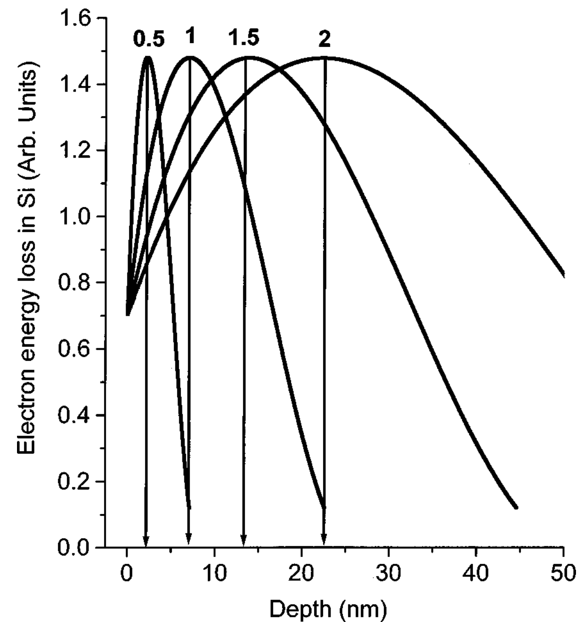

FIG. 1. Depth-dose curves of various electron beam energies for Si at an incident angle of 45° to the surface. While the total range for electron energy loss rapidly exceeds 5.0 nm, the maximum in the energy loss curve increases more slowly, reaching a maximum at 5 nm at a beam energy of ≈750 eV.

beam in kV. Using this relation to define the total range in combination with the general form for the electron energy loss curve as given by Everhart and Hoff,[11] we obtain an expression for the electron energy loss per unit path length as a function of depth for a given initial primary beam energy at normal incidence. A cos θ term takes the orientation of the electron gun relative to the specimen into account. Then, using a density for silicon of 2.33 g/cm^3,[12] we arrive at the form for the electron energy loss curve for a given initial beam energy as a function of depth and presented in Fig. 1. This figure shows how penetration increases with beam voltage and illustrates the wide range of excitation depths possible.

IV. RESULTS

Cathodoluminescence spectra as a function of probe depth are shown in Fig. 2 for the as-deposited specimen using the S-20 photomultiplier. The S-20 detector is sensitive above ≈1.4 eV on the low-energy end, while on the high-energy end of the spectrum, the spectra are cut off by the response of the monochromator at ≈3.75 eV. For high electron beam energies, the electrons easily penetrate past the 5 nm oxide overlayer into the bulk *p*-Si(100) substrate. The optical spectrum is dominated by a broad feature beginning from the detector cutoff at 1.5 eV extending out to 3.0 eV, while in the ultraviolet (UV) spectral region, a second unresolved feature is also observed, centered at 3.4 eV. As the electron beam energy is lowered to 2.0 kV, the 3.4 eV feature disappears. At still lower beam energies, a new feature appears at 2.7 eV, so that by 0.6 kV, the 2.7 eV feature is 80% of the intensity of the lower-energy feature centered at 1.9 eV. In

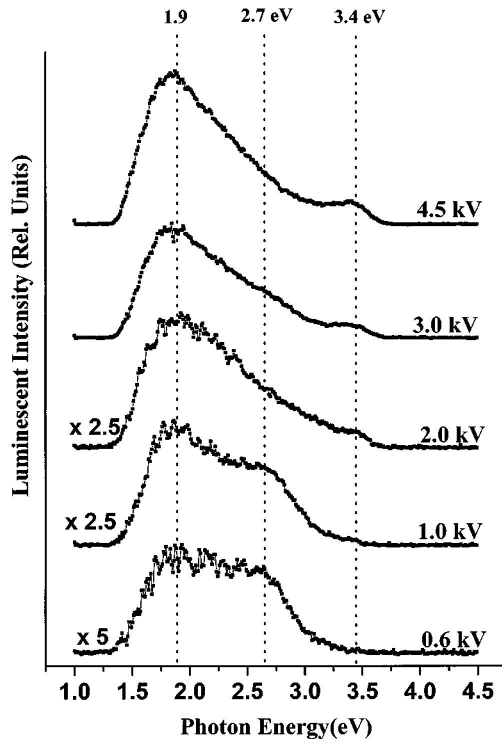

FIG. 2. CLS spectra of the as-deposited ultrathin 5 nm nitrided, SiO_2 film with a S-20 photodetector for varying incident electron beam energy. Close to the film/substrate interface (low excitation energies), defects characteristic of oxygen deficient SiO_x are detected at 2.7 eV. Evidence for direct transitions involving the Si substrate (3.4 eV) appears at higher beam energies.

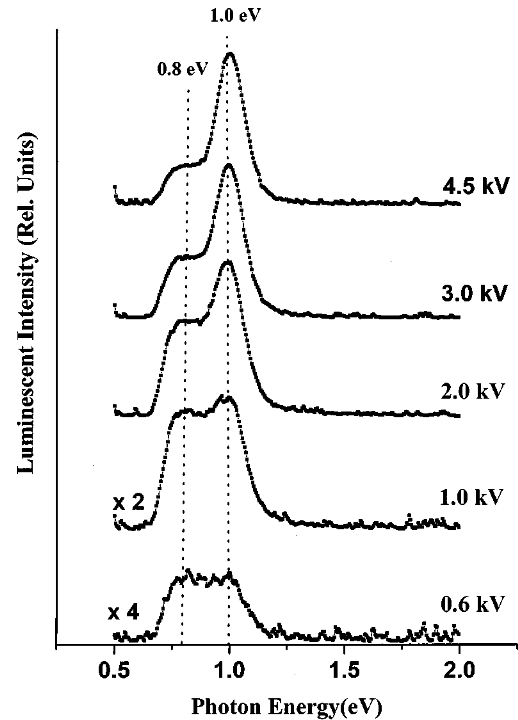

FIG. 3. CLS spectra of the as-deposited SiO_2–Si film in the infrared regime using a LN_2 cooled Ge detector. Si defect emission is evident at 0.8 eV. Band edge luminescence from the crystalline substrate increases with increasing excitation beam voltage and hence increasing excitation depth.

addition to the relative changes occurring between the two peaks, the overall optical intensity is decreasing, even though the same power is being injected into the specimen. The 0.6 kV spectrum is five times weaker than the corresponding 4.5 kV spectrum indicative of competition from surface nonradiative recombination channels.

As high-energy electrons thermalize within the silicon substrate, radiative recombination occurs between the lowest conduction band minimum and the valence band edge, i.e., the band gap. Indeed, depth-dependent CLS in the near infrared, shown in Fig. 3, indicates the presence of band gap related emission from the underlying Si at 1.0 eV for large penetration depths. In addition to the main feature at 1.0 eV, there is also spectral intensity centered near 0.8 eV. As the penetration depth of the primary electrons decreases, the band edge feature decreases leading to a relative increase in the 0.8 eV feature until, for the most shallow penetration depth (0.6 kV), the two features are of equal intensity.

V. PROCESS DEPENDENCE OBSERVED BY CLS

The CLS spectra observed at a beam energy of 1.0 kV highlights the changes occurring near the SiO_2–Si interface. Figure 4, the as-deposited spectra from Figs. 2 and 3 are replotted with the addition of the changes observed after various processing steps. Focusing first on the optical feature at 2.7 eV, we observe a 10% reduction in the luminescence intensity at this energy after the 400 °C hydrogenation processing step. The 900 °C RTA anneal is even more effective at reducing the intensity of this feature. Finally, the combination of the processing steps reduces the intensity to such an extent (over 40% from the as-deposited case) that it can no longer be resolved as a shoulder on the background.

In the infrared spectral region, the situation is more complicated. The 400 °C hydrogenation reduces both features at 0.8 and 1.0 eV. The 900 °C RTA anneal seems to have a similar effect on the specimen, reducing the intensity of both features by about a factor of 2. However, the combination of the two processing steps clearly increases the intensity from both features, basically to the same intensity level as the as-deposited case.

By taking advantage of the depth resolution capability of CLS, we can simultaneous compare and contrast the changes induced by processing in the substrate versus those at the interface. In Fig. 5, we show CLS spectra at a beam energy of 3 kV. From the curves in Fig. 1, the bulk of the electron-hole pair generation is clearly within the substrate when the beam energy is 3 kV. From the series of spectra at 3 kV in Fig. 5, we see the 400 °C anneal has little effect on the specimen in the infrared, while seeming to have the largest effect on the broad emission band between 1.5 and 2.5 eV, cutting the intensity in that spectral range significantly. On the other hand, the 900 °C RTA anneal has a large effect on the infrared part of the spectrum, cutting the 1.0 eV feature by a factor of 2, while at the same time having little or no effect at higher energies.

The combination of the 400 °C hydrogenation and the

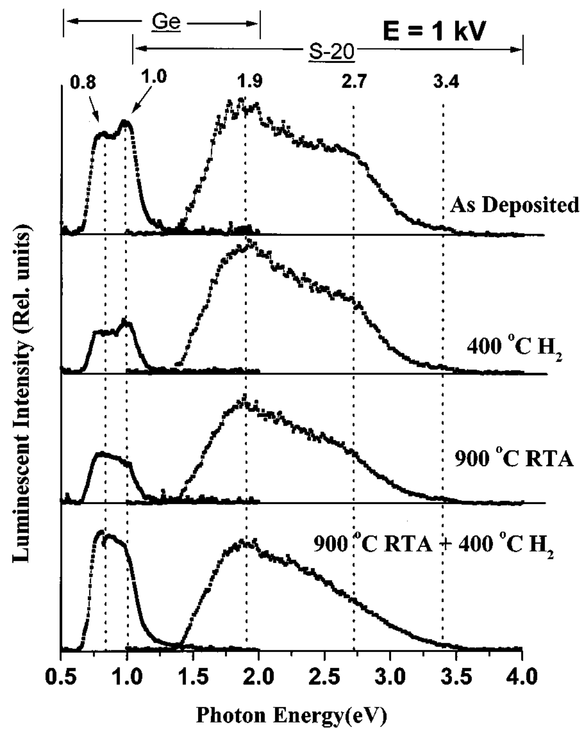

FIG. 4. Evolution of the defect bands vs annealing treatments for the same 1.0 kV electron beam excitation energy. The luminescent intensity for each detector is calibrated between scans. However, the absolute luminescent intensity response between the two detectors is not calibrated. A steady decrease in defect intensity is observed at 2.7 eV upon annealing. While in comparison, in the infrared, hydrogenation at 400 °C and the 900 °C RTA anneal reduce the luminescence features, the combination of the two anneals does not change the spectra appreciably.

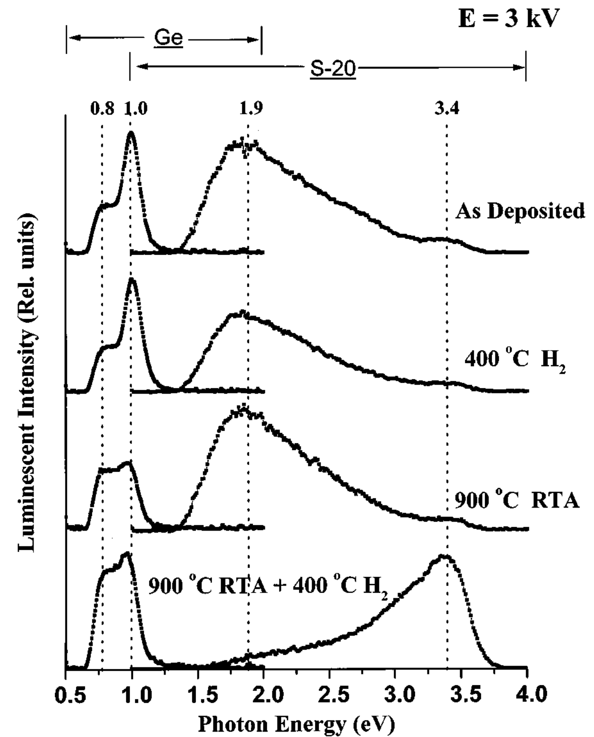

FIG. 5. Evolution of the defect bands vs annealing treatments for the same 3.0 kV excitation energy. The luminescent intensity for each detector is calibrated between scans. However, the absolute luminescent intensity response between the two detectors is not calibrated. A dramatic decrease in luminescence is observed for the band peaked at 1.9 eV upon annealing both with a 900 °C RTA anneal and with a 400 °C hydrogenation anneal. In the infrared though, the combination anneal actually increases the luminescent intensity at 0.8 eV.

900 °C RTA has a dramatic effect on all parts of the substrate CLS spectrum. In the optical and near-UV spectrum, the broadband from 1.5–2.5 eV is significantly reduced, with the main feature now centered at 3.4 eV, a feature barely observed in the as-deposited specimen. Furthermore, similar to the interface CLS spectrum in Fig. 4, the overall optical intensity in the infrared seems to have increased for the combination anneal relative to the individual anneals.

VI. DISCUSSION

The depth-dependent CLS spectra shows various aspects of the known luminescence spectra of the Si substrate and the SiO_2 overlayer. However, the possible effect on the spectra of a deliberately nitrided interface is not nearly as well understood. Amorphous SiO_2 has been shown to have two spectral features in the visible region of the spectrum,[13] one at 1.9 eV and the other at 2.7 eV, the main spectral feature occurring at 2.7 eV. These features are also observed in crystalline SiO_2 (quartz) indicating the localized nature of these optically active deep level defects. The 1.9 eV feature in SiO_2 has been correlated with the presence of hydroxyl groups in the SiO_2.[14] Since the bulk of the SiO_2 in our case is grown by RPECVD, which contains large amounts of ambient H during the growth process, one would expect to see some luminescence in the CLS spectral also at 1.9 eV.

Second, the feature at 2.7 eV has not only been seen in bulk SiO_2, but it has also been observed in thick, thermally grown SiO_2–Si films by CLs as well.[15] Furthermore, using etch-back techniques, the authors were able to determine that the 2.7 eV was localized within 25 nm of the interface of these thermally grown SiO_2–Si films. In previous work on non-nitrided SiO_2–Si,[4,5] we have been able to determine nondestructively that the 2.7 eV feature is within only a few nm of the interface.

Superimposed on the SiO_2-like features are the spectral features associated with the band structure of silicon as well as localized defects within the silicon itself. While bulk silicon does not luminescence strongly under laser excitation, it does luminescences under electron excitation at room temperature.[16] Si has two peaks in the imaginary component of the dielectric constant above the 1.1 eV band gap at 3.4 and 4.3 eV, respectively,[17] therefore, optical emission would also be expected at similar energies. While we cannot measure the 4.3 eV peak due to the low efficiency of this particular optical train, in the UV we can correlate the emission observed at 3.4 eV with the emission of light from bulk crystalline Si.

Localized defects both within the Si substrate and at the SiO_2–Si interface can lead to emission at below band-gap energies. Indeed, luminescence has been observed well be-

low the Si band gap at 0.8 eV (Ref. 18) and associated with Si dangling bonds. Broad above band-gap emission observed in 5 nm SiO_2–Si films and in these nitrided SiO_2–Si case is more difficult to explain. Because the emission at 1.5–2.5 eV is removed by the combination anneal shown in Fig. 5, it cannot be an intrinsic property of the substrate, therefore, this emission must be associated with local disorder in the silicon substrate in the near-interface region.

VII. ROLE OF N MONOLAYERS ON CLS SPECTRA

All spectral features mentioned in the previous section were also observed in 5 nm SiO_2–Si without the monolayer (ML) of N. The 1 ML N layer does not induce new optically active peaks in the CLS spectrum, however, it does have a dramatic impact on the process dependence behavior of these 5 nm films.

Beginning in the infrared, the 0.8 eV defect feature was observed to double in intensity after the combination anneals for the nitrided case. This is in stark contrast with the SiO_2–Si case, where the 0.8 and 1.0 eV features both decreased to very low intensities after the combination anneal. If the 0.8 eV feature is due to Si dangling bond defects, known to be passivated by H, then the N is preventing the passivation of these defects. Similarly, for the SiO_2–Si case, the broad disorder-induced emission at 1.5–2.5 eV was suppressed by the 900 °C RTA anneal alone[5] at $E=2$ kV, close to the interface. For the nitrided interface, both anneals are necessary. Furthermore, the emission is then only reduced at 3 kV, significantly further from the interface than in the non-nitrided case.

Speculating on the nature of this process dependence, N–N bond strengths are significantly higher (226 kcal/mol) than O–O bond strengths (119 kcal/mol), while Si–N bond (105 kcal/mol) are less than Si–O bonds at 190 kcal/mol.[19] While we do not know the precise bonding environment of the N in these films, it is clear they show enhanced luminescence compared to non-nitrided specimens, therefore, the nitrogen has not found it's optimal bonding configuration. The process parameters used in these experiments work extremely well for the SiO_2–Si interface, however, they may not be adequate for optimizing optical properties in the presence of nitrogen. The electrical properties of these nitrided films show great promise for MOS structures. From a kinetic standpoint, higher temperatures might be needed to complete any chemical reaction at the interface. All else being equal, higher temperature or longer time anneals might improve them further still.

In summary, we report observations of depth-resolved CLS interfacial regions and localized point defect arrangements for ultrathin, atomically controlled, nitrided SiO_2–Si films. While we do not directly observe the spectroscopic presence of nitrogen at the interface, it is clear the nitrogen dramatically alters the annealing behavior of these ultrathin films. The direct, nondestructive observation of the bonding arrangements both at and *below* the interface can help guide the future development of novel, ultrathin dielectrics.

ACKNOWLEDGMENTS

This work was sponsored in part by the NSF, Grant No. DMR 9711851 at the Ohio State University, and by the ONR, SRC, and the NSF Engineering Research Center at North Carolina State University.

[1]D. A. Buchanan and S.-H. Lo, in *The Physics and Chemistry of SiO₂ and the SiO₂–Si Interface*, edited by H. Z. Massoud, E. H. Poindexter, and C. R. Helms (Electrochemical Society, Pennington, NJ, 1996), pp. 319–322.

[2]G. Lucovsky, A. Banerjee, B. Hinds, B. Claflin, K. Kon, and H. Yang, J. Vac. Sci. Technol. B **15**, 1074 (1997).

[3]G. Lucovsky, Z. Jing, and D. R. Lee, J. Vac. Sci. Technol. B **14**, 2832 (1996).

[4]A. P. Young, J. Schäfer, G. Jessen, R. Bandu, L. J. Brillson, H. Niimi, and G. Lucovsky, J. Vac. Sci. Technol. B **16**, 2177 (1998).

[5]J. Schäfer, A. P. Young, L. J. Brillson, H. Niimi, and G. Lucovsky, Appl. Phys. Lett. **73**, 791 (1998).

[6]D. R. Lee, G. Lucovsky, M. S. Denker, and C. Magee, J. Vac. Sci. Technol. B **13**, 1788 (1995).

[7]T. Yasuda, Y. Ma, S. Habermehl, and G. Lucovsky, Appl. Phys. Lett. **60**, 434 (1992).

[8]S. V. Hattangady, R. G. Alley, G. G. Fountain, R. J. Markunas, G. Lucovsky, and D. Temple, J. Appl. Phys. **73**, 7635 (1993).

[9]D. R. Lee, G. Lucovsky, M. S. Denker, and C. Magee, J. Vac. Sci. Technol. A **13**, 1671 (1995).

[10]B. Yacobi and D. Holt, in *Cathodoluminescence Microscopy of Inorganic Solids* (Plenum, New York, 1990), p. 58.

[11]T. E. Everhart and P. H. Hoff, J. Appl. Phys. **42**, 5837 (1971).

[12]*Handbook of Chemistry and Physics*, 62nd ed. (CRC Press, Boca Raton, FL, 1981), p. B-37.

[13]M. A. Stevens Kalceff and M. R. Phillips, Phys. Rev. B **52**, 3122 (1995).

[14]H. Koyama, K. Matsubara, and M. Mouri, J. Appl. Phys. **48**, 5380 (1977).

[15]J. P. Mitchell and D. G. Denure, Solid-State Electron. **16**, 825 (1973).

[16]L. Hao, B. Hou, B. Yang, and X. Xu, Phys. Rev. B **57**, 12841 (1998).

[17]D. E. Aspnes and A. A. Studna, Phys. Rev. B **27**, 985 (1983).

[18]G. Lucovsky and S. Y. Lin, in *Optical Effects in Semiconductors*, edited by P. C. Taylor and S. G. Bishop [AIP Conf. Proc. **120**, 55 (1984)].

[19]*Handbook of Chemistry and Physics*, 62nd ed. (CRC Press, Boca Raton, FL, 1981), p. F-180.